2014 IEEE International Conference on Robotics & Automation (ICRA)
Hong Kong Convention and Exhibition Center
May 31 - June 7, 2014. Hong Kong, China

Towards Robot-Assisted Vitreoretinal Surgery: Force-Sensing Micro-Forceps Integrated with a Handheld Micromanipulator*

Berk Gonenc, *Student Member, IEEE*, Ellen Feldman, *Student Member, IEEE*, Peter Gehlbach, *Member, IEEE*
James Handa, Russell H. Taylor, *Fellow Member, IEEE*, and Iulian Iordachita, *Member, IEEE*

***Abstract*— In vitreoretinal practice, controlled tremor-free motion and limitation of applied forces to the retina are two highly desired features. This study addresses both requirements with a new integrated system: a force-sensing motorized micro-forceps combined with an active tremor-canceling handheld micromanipulator, known as Micron. The micro-forceps is a 20 Ga instrument that is mechanically decoupled from its handle and senses the transverse forces at its tip with an accuracy of 0.3 mN. Membrane peeling trials on a bandage phantom revealed a 60-95% reduction in the 2-20 Hz band in both the tip force and position spectra, while peeling forces remained below the set safety threshold.**

I. Introduction

Retinal microsurgery ranks among the most challenging areas of surgical practice, requiring the manipulation of extremely delicate tissues by various micron scale maneuvers and the application of very small forces. Among vitreoretinal procedures, membrane peeling is a standard task in which a very thin fibrous membrane on the retina surface is delaminated, either by using a pick or micro-forceps. During this operation, instruments need to be moved relatively slowly, within a range of 0.1–0.5 mm/s. Furthermore, the required forces for delamination routinely lie below the surgeon's sensory threshold. Most of these forces were shown to be below 7.5 mN in porcine cadaver eyes, and only 19% of events with this force magnitude can be felt by surgeons [1]. In manual practice, surgeons generally lack tactile responses or force feedback, and rely largely on visual cues. They visually monitor local surface deformation and adjust peeling speed in order to prevent application of excessive forces, which can give rise to serious complications such as iatrogenic retinal breaks [2], vitreous hemorrhage, and subretinal hemorrhage [3]. This task is extremely challenging and depends upon extensive experience, considering the other factors involved in the procedure, which include poor visualization, inconsistent tissue properties, physiological hand tremor of the surgeon, fatigue and patient motion. Assistive systems which both eliminate tremor from tool motion and limit applied forces could be a significant solution in addressing these challenges and thus improve surgical outcomes.

In order to reduce physiological hand tremor, provide fine motion control, and consequently enhance microsurgical accuracy, several teleoperated robotic systems have been developed by different researchers [4-9]. In contrast to these approaches, the Steady-Hand Robot developed at the Johns Hopkins University (JHU) is based upon a cooperative control scheme between the surgeon and a stiff non-backdrivable robotic arm [10]. Micron was designed as a fully-handheld micromanipulator by Riviere et al. at Carnegie Mellon University [11].

Focusing on the lack of force feedback, a family of force-sensing instruments was developed at JHU using fiber Bragg grating (FBG) strain sensors to measure the forces directly at the tool tip. First, a single degree of freedom (DOF) force-sensing tool [12] and then a 2-DOF pick-like instrument [13] were built with FBG sensors. The 2-DOF pick was used in combination with the Steady-Hand Robot [14] as well as with Micron [15]. Compared with a pick tool, forceps provide increased control due to the additional degree of freedom for grasping the tissue. This enables removal of the membrane from the eye in a single step [16], which is why forceps are more practical and more commonly used in vitreoretinal surgery. With this motivation, tool development continued with a manual pair of 2-DOF force-sensing forceps [17], followed by a 2-DOF forceps that can be used with the Steady-Hand Robot [18]. These can sense only the transverse tool-to-tissue interaction forces, which is a limitation for practical use in membrane peeling. For this reason, the design concept of a 3-DOF force-sensing forceps compatible with the Steady-Hand Robot was proposed, but is challenged by the available fabrication techniques [19].

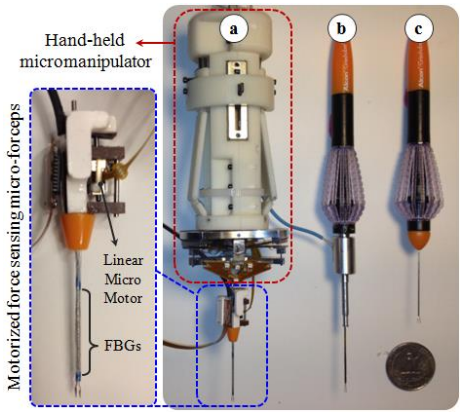

Figure 1. (a) Motorized force-sensing micro-forceps integrated with a handheld micromanipulator (Micron), (b) 2-DOF force-sensing micro-forceps for the Steady-Hand Robot [18] (c) Original 23Ga disposable forceps (Alcon, USA).

*Research supported in part by the National Institutes of Health under R01 EB007969, and R01 EB000526, and in part by Johns Hopkins University internal funds.

B. Gonenc, R. H. Taylor, and I. Iordachita are with CISST ERC at Johns Hopkins University, Baltimore, MD 21218 USA (e-mail: bgonenc1,rht,iordachita@jhu.edu) (Corresponding author: Berk Gonenc, phone: 360-975-1676; e-mail: bgonenc1@jhu.edu).

J. Handa and P. Gehlbach are with the Wilmer Eye Institute at The Johns Hopkins School of Medicine, Baltimore, MD 21287 USA (e-mail: jthanda,pgelbach@jhmi.edu)

E. Feldman is with Viterbi School of Engineering at the University of Southern California, Los Angeles CA, 90089, USA (e-mail: erfeldma@usc.edu)

Integrating the developed force-sensing tools with the Steady-Hand Robot and Micron forms two distinctly different assistive systems that can address both tremor and force limitation problems in membrane peeling. In our recent comparison study [20], we evaluated membrane peeling performance using these systems with the latest available force-sensing tool for each manipulator: a 2-DOF forceps for the Steady-Hand Robot, and a 2-DOF pick for Micron. Results showed that Micron performance was significantly challenged by the lack of a forceps tool for this system. Using the micro-forceps with the Steady-Hand Robot has revealed superior performance, as one can hold the tissue firmly and manipulate it more easily without slippage. In order to improve Micron's performance in this task and to make a fair comparison between the two assistive systems, it is crucial to have a compact lightweight force-sensing forceps module. In comparison to a manual or Steady–Hand Robot compatible forceps, this presents a completely different design problem with much stricter constraints.

In this paper, we report a new integrated assistive system for membrane peeling, combining an active tremor-canceling handheld micromanipulator with a force-sensing motorized micro-forceps. In the following sections, we will first present the design and calibration of our new force-sensing tool. This will be followed by system integration steps and the results of peeling experiments on a bandage phantom. The paper concludes with a discussion of the results.

II. Motorized Force-Sensing Micro-Forceps

A. Design

The design of the force-sensing micro-forceps includes two main parts: the handle mechanism (Fig 2.a), and the motorized force-sensing tip (Fig. 2.b and c).

For the handle mechanism, it is desirable to preserve the intuitive actuation mechanism on the existing disposable forceps from Alcon, Inc. (Fort Worth, TX), which was also used in our previous force-sensing micro-forceps for the Steady-Hand Robot [18]. This mechanism can be actuated simply by squeezing the tool handle. The squeezing motion causes the tube forming the tool shaft to slide in the distal direction to close the graspers. In our case, however, such rigid coupling between handle motion and tip actuation is not possible, since it would significantly interfere with the handheld micromanipulator's actuators. Instead of such a mechanical coupling, we used a sliding potentiometer on the handle to assess forceps closure. The sides of the handle mechanism are normally kept propped open by two springs as shown in Fig 2.a. Compressing the sides causes the sliders to move up along the tool handle (see the video attachment), inducing a voltage change in the potentiometer output. With the help of set screws, this mechanism can clamp onto any cylindrical manipulator handpiece up to 25 mm in diameter, transforming it into a micro-forceps handle.

In designing the motorized force-sensing tip, three main challenges needed to be overcome: (1) integrating force sensing capabilities while preserving the grasping motion of forceps, (2) avoiding interference between the manipulator's own actuation and the opening/closing action of the forceps, and (3) generating a self-standing universal module for compatibility with various handheld manipulators. This requires a very compact and lightweight micro-forceps module that can be actuated independently of the attachment site on the micromanipulator, and that carries all the force-sensing elements on it. Under these constraints we designed our "drop-in" micro-forceps as shown in Fig. 2.b and Fig. 2.c.

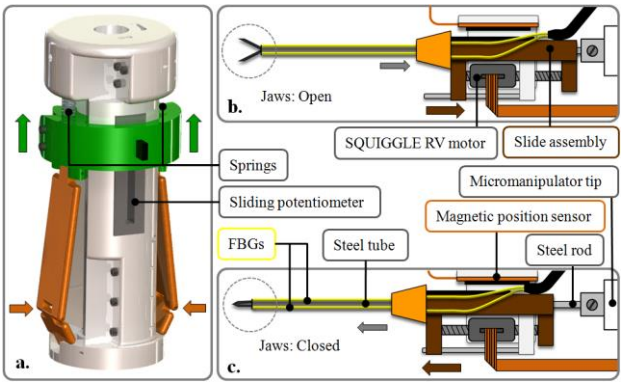

Figure 2. Design of force-sensing micro-forceps for handheld micromanipulators: (a) handle mechanism (b,c) motorized force-sensing tip. Squeezing the handle mechanism from the sides drives the motor and pushes the slide assembly forward, and thus closes the grasper jaws.

In this concept, the forceps jaws are normally open, and are rigidly attached to the proximal end of the module by a steel rod. This rod lies along the whole tool, initially passing through a 23 gauge (Ga) steel tube in the distal end, and then through the sliding assembly in the proximal end. The 23 Ga stainless steel tube is rigidly attached to the slide assembly. For actuation, a linear micro motor, Squiggle-RV-1.8 by New Scale Technologies Inc., was selected due to its small size (2.8x2.8x6 mm), light weight (0.16 grams), precision (0.5 μm resolution), and high force (up to 0.33 N). The shaft of the motor is housed by the slide assembly at both ends to move it back and forth along the steel rod for opening and closing the forceps jaws (see the video attachment). This requires a travel distance of 1.2 mm, which is well below the motor's limit (6mm). The position is tracked via the NSE-5310 magnetic position sensor located on the side of the slide assembly for closed-loop control. To integrate force sensing capabilities, FBG strain sensors (Smart Fibers, UK) were preferred mainly due to their small dimension, high sensitivity, biocompatibility, sterilizability, and immunity from electrostatic and electromagnetic noise. Following the fabrication method presented in [13], 3 FBGs were fixed on the 23 Ga tubular tool shaft axisymmetrically using medical epoxy adhesive. In order to monitor the FBGs, an optical sensing interrogator, sm130-700 from Micron Optics Inc. (Atlanta GA), was used. The outer diameter of the finalized tool shaft is approximately 0.9 mm, and is small enough to fit through a 20 Ga trocar. The module weighs less than 2 grams.

B. Calibration and Force Computation

The calibration setup and protocol of the new micro-forceps module follow [13]. A linear reproducible behavior was observed for all FBGs during both the x- and y-axis calibration procedures, as shown in Fig. 3.

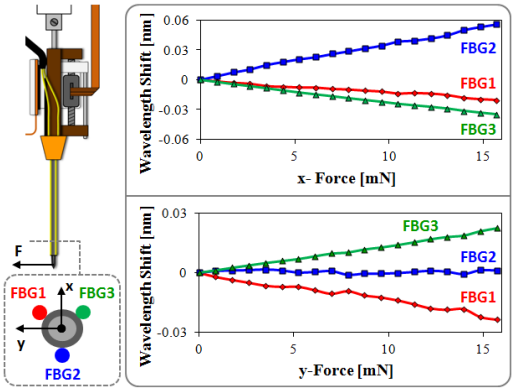

Figure 3. Calibration results in x-axis direction (upper) and in y-axis direction (lower). Linear behavior is observed for all FBGs in both axes.

Based on the results in Fig. 3, the following calibration matrix was determined:

$$K = \begin{bmatrix} 0.01084 & 0.01394 \\ -0.03276 & 0.00016 \\ 0.02192 & -0.01410 \end{bmatrix}$$

To compute the tip forces (F) from FBG wavelength shift (ΔS), the pseudo-inverse of the obtained calibration matrix (K^{+}) is used in the linear relationship given by (1) This algorithm was previously shown to effectively remove the influence of ambient temperature [13].

$$F = K^{+} \Delta S \qquad (1)$$

The steel tube forming the tool shaft in our design is not only a functional element that provides the grasping action, but is also a structural element that carries the force-sensing FBGs. As the grasper jaws are squeezed and released, various external loads and frictional forces are induced on this tube. FBGs sense a combination of these inner actuation forces and the tip forces. The result is a repeated and consistent shift in force readings as the forceps is closed and opened even when there is no loading on the tip. This is highly undesirable as the maximum amount of shift (around 1 mN for each transverse force as in Fig. 4) is comparable to the amplitude of most forces during vitreoretinal practice (routinely below 7.5 mN).

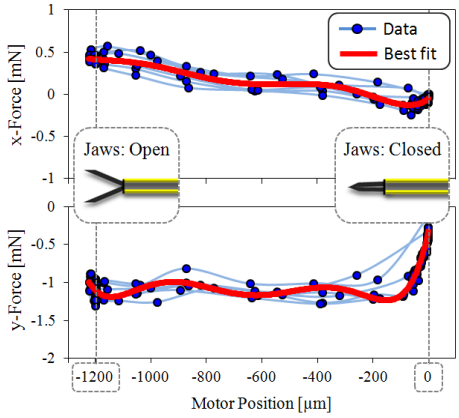

Figure 4. Measured forces vs. the motor position while no external force is applied on the forceps tip. Varying nonzero forces are observed as the grasper jaws are opened and closed due to inner actuation forces. Best fit curve is used to compensate for this effect.

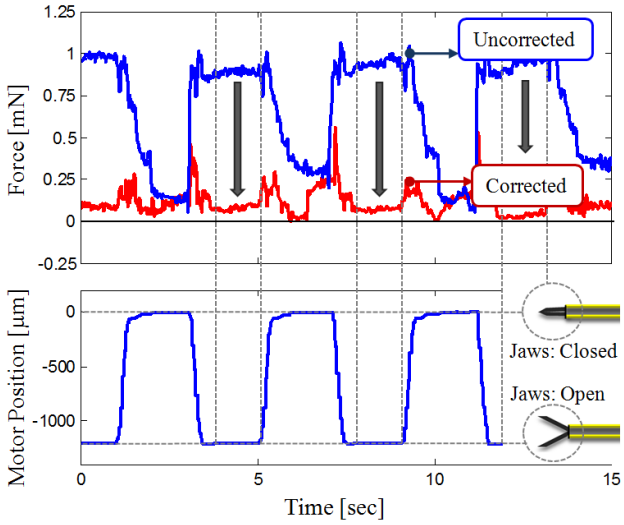

Figure 5. Consistent cycles of shift in force as the forceps is opened and closed repeatedly. The max. amplitude of this change is reduced from 1mN to 0.3 mN after correction based on motor position.

In order to model and compensate for this effect, we recorded the force variation with no force applied to the tip during 3 consecutive opening-closing cycles, which resulted in the mapping shown in Fig. 4. Due to grasper jaw geometry, material properties, and the frictional forces between the steel tube and forceps jaws, the behavior in Fig. 4 is highly nonlinear, yet consistent. This mapping relates the actuation forces to the motor position within ±0.15mN. Based on the identified best fit and sensed motor position, the induced forces due to actuation can be estimated and subtracted from the measured values to obtain a corrected force reading. This provides a significant reduction in force variation as the forceps is closed and opened repeatedly. As shown in Fig. 5, without such correction, the maximum force change is around 1 mN while the correction reduces it to 0.3 mN. This indicates that our tool is able to measure the forces in any direction in the xy-plane with an accuracy of 0.3 mN.

III. System Integration and Control Scheme

In order to form a complete assistive system for membrane peeling, the elements of the motorized force-sensing micro-forceps were integrated with a handheld micromanipulator, Micron. This device is able to cancel physiological hand tremor by activating three piezoelectric actuators. The position of its handle is determined by ASAP optical sensors [11]. After sensing the tool motion, Micron separates it into involuntary and tremorous components. Then Micron moves its tip to counteract the involuntary motion component within a workspace of approximately a 1x1x0.5 mm volume centered on the handle position. The control software for tremor cancellation was implemented in LabVIEW as shown in Fig. 6.

The designed motorized micro-forceps module was mounted on the micromanipulator tip. Micron has about 1 N force capability, which is enough to support and move this additional load (smaller than 2 grams) quickly for effective tremor compensation. Hardware implementations were completed by clamping on the designed handle mechanism

to transform the Micron handpiece into a forceps-handle. The control loop associated with the actuation of the forceps is shown in green in Fig.6. Accordingly, analog position servo input is provided to the Squiggle motor controller via the sliding potentiometer on the handle mechanism. The magnetic sensor on the forceps tip provides position feedback to accomplish accurate closed loop control, opening or closing the grasper jaws without noticeable delay.

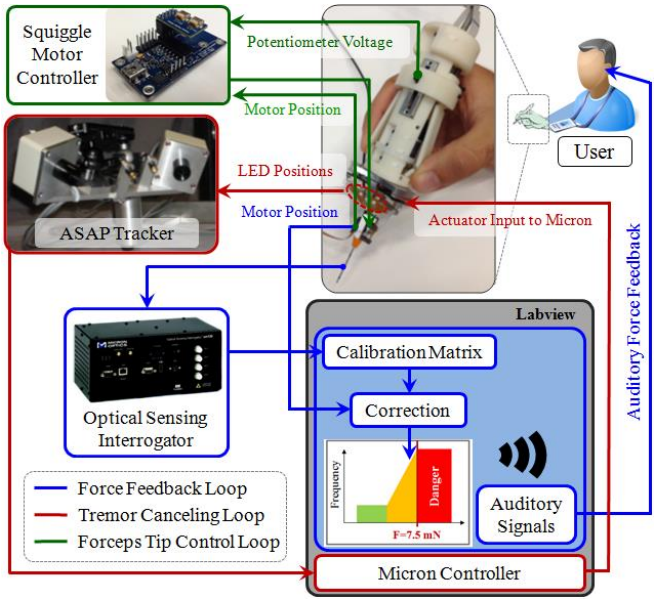

Figure 6. The control scheme of the integrated system. Accompanying the existing tremor canceling control loop, two more branches were added to provide auditory force feedback and to control forceps jaws by squeezing the handle.

The existing LabVIEW control software was extended to include a force feedback loop as shown in blue in Fig. 6. During operation, the wavelength information from each FBG channel is collected and processed at 1 kHz and transmitted over TCP/IP to the LabVIEW environment. Forces are then computed utilizing the calibration matrix. Based on forceps configuration (linear motor position), the computed force value is corrected to obtain tip forces. These tip forces are then converted into auditory signals. The frequency of these audio signals changes with the level of the applied force [14]. Depending on the frequency of the auditory feedback (AF), the user adjusts tool motion so that the applied forces do not exceed 7.5 mN, which we define as the danger zone threshold in membrane peeling based upon our prior in-vivo experience [17].

IV. Experiments

In order to assess the performance of the developed system, several peeling trials were performed by a single non-surgeon subject on the setup shown in Fig 7. As a surrogate for epiretinal membrane, 2 mm wide strips were cut from 19 mm Clear Bandages (RiteAid brand), which have previously been reported and used in our laboratory for similar tests [14, 20]. The bandage strips were attached to a plastic base with curvature (Ø 25 mm) resembling the back of the eye. In addition, a rubber sclerotomy constraint was located directly above the bandage strips.

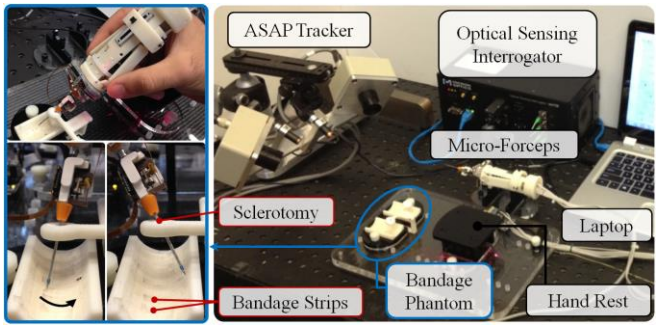

Figure 7. Setup for membrane peeling experiments on bandage phantom.

During the experiment, the subject was asked to (1) insert the micro-forceps tool through the sclerotomy point, (2) grasp and lift the bandage edge, and (3) peel the strip off of the plastic surface while keeping the tool velocity as uniform as possible (~0.5 mm/s) and the delaminating forces below the danger threshold (~7.5 mN) based on the provided auditory force feedback. The goal of the experiment is to identify any interference between the micro-forceps and Micron operation, and to determine whether the implemented hardware modifications affect the device's tremor canceling characteristics. For this reason, the experiments were done in two sets by turning the tremor cancellation feature on and off. Five peels were recorded per category, and the tests were performed in alternating order. Before data collection, an extensive training period (~1 hrs) was allowed for the subject to become accustomed to the system and phantom, and to minimize learning curve effects in the recorded measurements. During data collection, the tool tip force and position and the Squiggle motor position were recorded. Based upon the Squiggle motor position, the starting and ending points of the delamination were identified in the acquired data. The assessment was based on the applied forces and tool tip positions during this period.

V. Results and Discussion

Measured forces on the bandage phantom are displayed for all trials in Fig. 8. The starting time of the task is set at the point when the user starts closing the grasper jaws. The delaminating period begins after the forceps are closed, and the forces after this time are of interest. During the delaminating period, the exerted forces in all trials remained below the safety threshold (7.5 mN), which displays the effectiveness of the auditory force feedback and agrees with our previous results [15, 20]. On the other hand, high frequency oscillations were visible when the tremor suppression feature of the system was not used. Upon activation of Micron, these oscillations were significantly reduced.

The effect of physiological hand tremor is also visible in velocity and tip position plots. In all trials, the user managed to keep the peeling speed around 0.5 mm/s as desired; however, oscillations and difficulty increased in the absence of Micron tremor aid. Fig. 9 shows that the tool tip in Micron-assisted trials followed a much smoother trajectory with higher positioning accuracy in comparison to the cases without tremor cancellation.

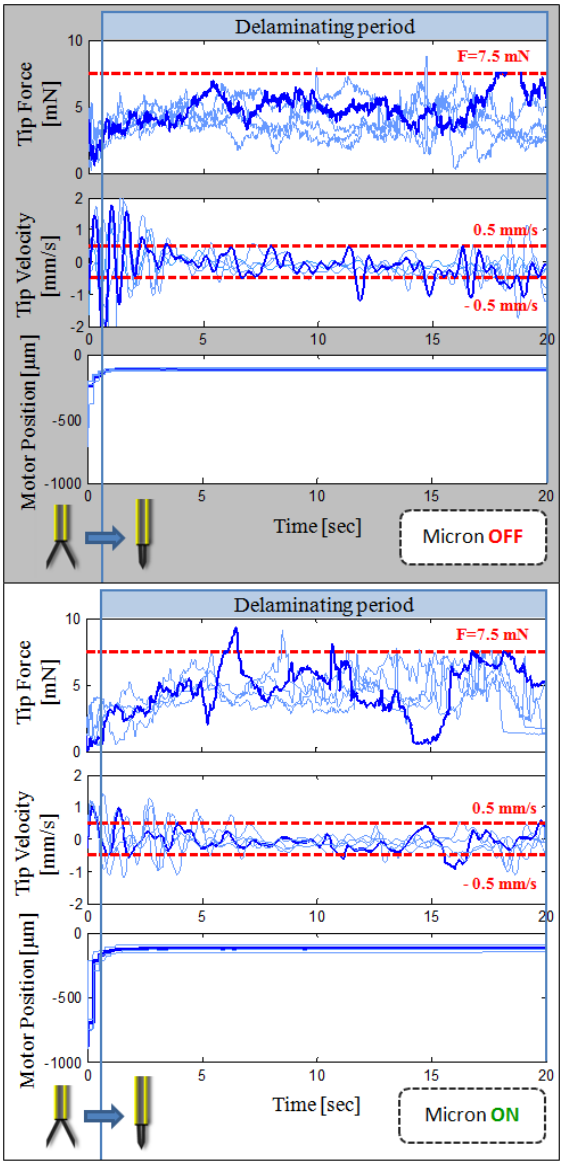

Figure 8. Measured peeling forces using bandage phantom for all trials (5 trials/case). One of the trials was shown in darker color to highlight the important characteristics. Auditory feedback helps in keeping forces below the safety threshold (7.5 mN). The peeling speed is kept below 0.5 mm/s successfully in all cases, but with much difficulty when Micron is off. The tremor canceling feature of Micron helps in reducing high frequency oscillations in both tip force and tip velocity.

In order to assess the tremor canceling effect of Micron in our tests, we performed frequency analyses based on both position and force measurements. The results are presented in Fig. 10. The bandwidth of human hand-eye feedback usually is from 0.5 Hz to 2 Hz [21]. Below 0.5 Hz, hand-eye feedback becomes effective. Thus, the regions below 0.5 Hz in these figures represent controlled actions, whereas frequencies above 2 Hz indicate the unintentional motion of the user. The postural hand tremor frequency in normal humans is approximately 8-10 Hz [21]. The prominence of a peak around 9 Hz in Micron-off trials is primarily due to the subject's hand tremor. When the tremor suppression feature is activated, this peak is eliminated and the high-frequency components (2-20 Hz) are overall reduced by 60-95% in both the tip force and tip position spectra.

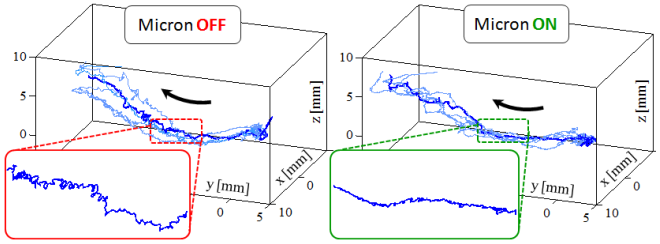

Figure 9. Tool tip trajectory during the delaminating period. The arrow indicates the peeling direction. Higher positioning accuracy and smoother paths are observed with Micron use.

The significant reduction in the 2-20 Hz band and percentages comparable to our previous results with Micron [15, 20] confirm that there is no adverse effect in tremor suppression characteristics due to the newly-introduced micro-forceps tip module. On the contrary, the forceps allow for grasping—and thus a more rigid connection between the tool tip and membrane—which now enables us to relate the characteristics of the measured forces to the tool tip dynamics. The common power spectral density traits in Fig. 9 strongly indicate this connection. Previously, when using the pick instrument, such direct comparison did not yield reliable results, especially during trials in biological phantoms such as chick embryos, due to slippage between the tool and the tissue [20]. Furthermore, with the new forceps tip, the user can accomplish the peeling task in a single attempt, whereas a pick instrument could necessitate multiple attempts due to associated challenges in tissue manipulation. This is not only important for ease of use, but also significantly increases safety, since multiple delamination attempts intensify the risk of retinal damage.

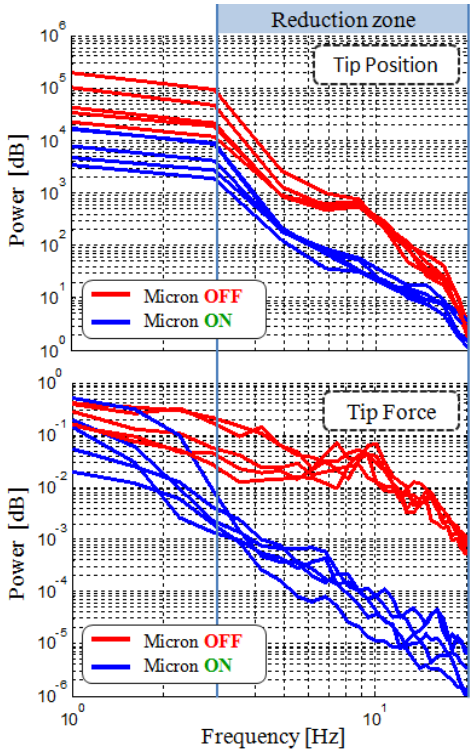

Figure 10. Frequency analysis on tip position and peeling forces. Highly correlated spectral density traits due to strong grasping provided by forceps use: a peak at 9 Hz due to physiological hand tremor and a 60-95% reduction in 2-20 Hz oscillations in both tip force and position spectra.

VI. CONCLUSION

This paper presents an integrated assistive system for membrane peeling that combines an active tremor-canceling handheld micromanipulator, Micron, with a force-sensing motorized micro-forceps. Our system addresses two of the most critical requirements of vitreoretinal surgery: tremor-free tool motion and limitation of applied forces.

In this study, we first developed a compact, lightweight, force-sensing micro-forceps module with an intuitive handle mechanism. The tip was motorized so that there is no mechanical coupling required between the handle mechanism and the forceps tip. Three FBGs were incorporated onto the tip module to provide 2-DOF force sensing capability with a resolution of 0.3 mN. In order to form a complete system, the module was integrated onto Micron. Membrane peeling tests were performed on a bandage phantom to monitor performance and identify any advantages or disadvantages regarding the integration. Analyses revealed no adverse effect upon Micron's performance due to the added inertia of the forceps module. Compared to a pick instrument, the micro-forceps provided an easier and safer operation by facilitating better tissue manipulation and enabling peeling to be accomplished in a single attempt. In addition, the slippage problem in pick usage was eliminated. Consequently the measured tool-to-tissue forces and tool-tip dynamics were more highly correlated.

The forceps tip used in this work is modified from a disposable tool. For this reason, the tip fails after a limited number of actuation cycles. We currently are following two different paths in parallel to solve this issue. The first solution is to modify the design so that the disposable jaws can easily be replaced with new ones. The second approach is to design permanent forceps jaws by eliminating the friction and wear in the current design. This would also allow for more accurate modeling and estimation of inner actuation forces, and consequently increased accuracy in force sensing. Upon developing a system that can endure prolonged use, we aim to extend our results through multiple-subject experiments.

ACKNOWLEDGMENT

The authors thank Prof. Cameron Riviere and his team at Carnegie Mellon University for providing the Micron robot, Alcon, Inc. (Fort Worth, TX) for their help with providing the micro-forceps tools, and Tom Guidarelli from New Scale Technologies, Inc. for assistance in hardware implementation.

REFERENCES

[1] P. Gupta, P. Jensen, and E. de Juan, "Surgical forces and tactile perception during retinal microsurgery," in *Proc. MICCAI'99*, 1999, pp. 1218–1225.

[2] R. N. Sjaarda, B. M. Glaser, J. T. Thompson, R. P. Murphy, and A. Hanham, "Distribution of iatrogenic retinal breaks in macular hole surgery," *Ophthalmology*, vol. 102:9, pp. 1387-1392, Sep. 1995.

[3] K. Nakata, M. Ohji, Y. Ikuno, S. Kusaka, F. Gomi, and Y. Tano, "Sub-retinal hemorrhage during internal limiting membrane peeling for a macular hole," *Graefes Arch Clin Exp Ophthalmol*, vol. 241, pp. 582-584, Jul. 2003.

[4] P. S. Schenker, E. C. Barlow, C. D. Boswell, H. Das, S. Lee, T. R. Ohm, E. D. Paljug, G. Rodriguez, and S. T. Charles, "Development of a telemanipulator for dexterity enhanced microsurgery," in *Proc. 2nd Int Symp Med Rob Comput Asst Surg*, 1995, pp. 81-88.

[5] I. W. Hunter, L. A. Jones, M. A. Sagar, S. R. Lafontaine, and P. J. Hunter, "Opthalmic microsurgical robot and associated virtual environment," *Comput Biol Med*, vol. 25:2, pp. 173-182, Mar. 1995.

[6] T. Ueta, Y. Yamaguchi, Y. Shirakawa, T. Nakano, R. Ideta, Y. Noda , A. Morita, R. Mochizuki, N. Sugita, M. Mituishi, and Y. Tamaki, "Robot-assisted vitreoretinal surgery: Development of a prototype and feasibility studies in an animal model," *Ophthalmology*, vol. 116:8, pp. 1538-1543, Aug. 2009.

[7] H. Das, H. Zak, J. Johnson, J. Crouch, and D. Frambach, "Evaluation of a telerobotic system to assist surgeons in microsurgery," *Comput Aided Surg* ,vol. 4:1, pp. 15-25, 1999.

[8] P.S. Jensen, K. W. Grace, R. Attariwala, J. E. Colgate, and M. R. Glucksberg, "Toward robot-assisted vascular microsurgery in the retina," *Graefes Arch Clin Exp Ophthalmol*, vol. 235:11, pp. 696-701, Nov. 1997.

[9] A. P. Mulgaonkar, J. P. Hubschman, J. L. Bourges , B. L. Jordan, C. Cham, J. T. Wilson, T. C. Tsao, and M. O. Culjat, "A prototype surgical manipulator for robotic intraocular micro surgery," *Stud Health Technol Inform*, vol. 142, pp. 215-217, 2009.

[10] A. Uneri, M. A. Balicki, J. Handa, P. Gehlbach, R. H. Taylor, and I. Iordachita, "New steady-hand Eye Robot with micro-force sensing for vitreoretinal surgery," in *Proc. 3rd IEEE RAS EMBS Int Conf Biomed Robot Biomechatron (BioRob)*, 2010, pp.814-819.

[11] R. A. MacLachlan, B. C. Becker, J. Cuevas Tabarés, G. W. Podnar, L. A. Lobes, and C. N. Riviere, "Micron: an actively stabilized handheld tool for microsurgery," *IEEE Trans Robot*, vol.28:1, pp.195-212, Feb. 2012.

[12] Z. Sun, M. Balicki, J. Kang, J. Handa, R. Taylor, and I. Iordachita, "Development and preliminary data of novel integrated optical micro-force sensing tools for retinal microsurgery," in *Proc. IEEE Int. Conf. on Robotics and Automation (ICRA '09)*, 2009, pp. 1897 –1902.

[13] I. Iordachita, Z. Sun, M. Balicki, J. Kang, S. Phee, J. Handa, P. Gehlbach, and R. Taylor, "A sub-millimetric, 0.25 mn resolution fully integrated fiber-optic force-sensing tool for retinal microsurgery," *International Journal of Computer Assisted Radiology and Surgery*, vol. 4, pp. 383–390, 2009.

[14] M. Balicki, A. Uneri, I. Iordachita, J. Handa, P. Gehlbach, and R. Taylor, "Micro-force Sensing in Robot Assisted Membrane Peeling for Vitreoretinal Surgery," *Med Image Comput Comput Assist Interv.*, vol. 13, pp. 303–310, 2010.

[15] B. Gonenc, M. A. Balicki, J. Handa, P. Gehlbach, C. N. Riviere, R. H. Taylor, and I. Iordachita, "Preliminary Evaluation of a Micro-Force Sensing Handheld Robot for Vitreoretinal Surgery, " in *Proc. IEEE Int. Conf. on Intelligent Robots and Systems (IROS '12)*, 2012, pp.4125-4130.

[16] S. Charles, "Techniques and tools for dissection of epiretinal membranes," *Graefe's Archive for Clinical and Experimental Ophthalmology*, vol. 241:5, pp. 347-352, 2003.

[17] X. He, M. A. Balicki, J. U. Kang, P. L. Gehlbach, J. T. Handa, R. H. Taylor, and I. I. Iordachita, "Force sensing micro-forceps with integrated fiber bragg grating for vitreoretinal surgery," in *Proc. of SPIE*, vol. 8218, pp. 82180W 1-7, Feb. 2012.

[18] I. Kuru, B. Gonenc, M. Balicki, J. Handa, P. Gehlbach, R. H. Taylor, and I. Iordachita, "Force Sensing Micro-Forceps for Robot Assisted Retinal Surgery," in *Proc. International Conference of the IEEE EMBS (EMBC '12)*, 2012, pp. 1401-1404.

[19] B. Gonenc, J. Handa, P. Gehlbach, R. H. Taylor, and I. Iordachita, "Design of 3-DOF Force Sensing Micro-Forceps for Robot Assisted Vitreoretinal Surgery," in *Proc. International Conference of the IEEE EMBS (EMBC '13)*, 2013, pp. 5686-5689.

[20] B. Gonenc, J. Handa, P. Gehlbach, R. H. Taylor, and I. Iordachita, "A Comparative Study for Robot Assisted Vitreoretinal Surgery: Micron vs. the Steady-Hand Robot," in *Proc. IEEE Int. Conf. on Robotics and Automation (ICRA '13)*, 2013, pp. 4832-4837.

[21] R. N. Stiles, "Mechanical and neural feedback factors in postural hand tremor of normal subjects," *J. Neurophysiol.*, vol. 44, pp. 40-59, Jul. 1980.